Downloaded from genesdev.cshlp.org on September 30, 2020 - Published by Cold Spring Harbor Laboratory Press

Yra1-bound RNA–DNA hybrids cause orientation-independent transcription–replication collisions and telomere instability

María García-Rubio,[1,3] Paula Aguilera,[2,3] Juan Lafuente-Barquero,[1] José F. Ruiz,[1] Marie-Noelle Simon,[2] Vincent Geli,[2] Ana G. Rondón,[1] and Andrés Aguilera[1]

[1]Andalusian Center of Molecular Biology and Regenerative Medicine (CABIMER), Universidad de Sevilla-Consejo Superior de Investigaciones Científicas (CSIC)-Universidad Pablo de Olavide, 41092 Seville, Spain; [2]Marseille Cancer Research Center (CRCM), U1068, Institut National de la Santé et de la Recherche Médicale (INSERM), UMR7258, Centre National de la Recherche Scientifique (CNRS), Aix Marseille University, Institut Paoli-Calmettes, Equipe Labellisée Ligue, 13273 Marseille, France

R loops are an important source of genome instability, largely due to their negative impact on replication progression. Yra1/ALY is an abundant RNA-binding factor conserved from yeast to humans and required for mRNA export, but its excess causes lethality and genome instability. Here, we show that, in addition to ssDNA and ssRNA, Yra1 binds RNA–DNA hybrids in vitro and, when artificially overexpressed, can be recruited to chromatin in an RNA–DNA hybrid-dependent manner, stabilizing R loops and converting them into replication obstacles in vivo. Importantly, an excess of Yra1 increases R-loop-mediated genome instability caused by transcription–replication collisions regardless of whether they are codirectional or head-on. It also induces telomere shortening in telomerase-negative cells and accelerates senescence, consistent with a defect in telomere replication. Our results indicate that RNA–DNA hybrids form transiently in cells regardless of replication and, after stabilization by excess Yra1, compromise genome integrity, in agreement with a two-step model of R-loop-mediated genome instability. This work opens new perspectives to understand transcription-associated genome instability in repair-deficient cells, including tumoral cells.

[*Keywords*: Yra1; R loop; transcription–replication collision; telomeres]

Supplemental material is available for this article.

Received December 28, 2017; revised version accepted May 16, 2018.

RNA–DNA hybrids are produced cotranscriptionally when the nascent transcript threads back hybridizing with the template DNA, leading together with the displaced nontemplate ssDNA to a structure termed the R loop. Hybrids have a tendency to accumulate preferentially at highly transcribed protein-coding genes, peaking at promoters and terminators, rDNA, tRNA-coding genes, Ty elements, centromeres, and telomeres (Ginno et al. 2012; Chan et al. 2014; El Hage et al. 2014; Wahba et al. 2016). RNA–DNA hybrids may benefit cell physiology, as shown in some cases of transcription initiation and termination, mitochondrial DNA replication, or immunoglobulin class switching (Aguilera and García-Muse 2012). However, RNA–DNA hybrids may also have a strong impact on genome instability, as shown in cells defective in specific mRNP assembly factors such as the THO complex or the SRSF1 RNA-binding protein, topoisomerase I, RNA–DNA helicases, or RNase H, a ribonuclease that specifically degrades the RNA moiety of RNA–DNA hybrids (Santos-Pereira and Aguilera 2015; Sollier and Cimprich 2015). Accumulating evidence indicates that most of this genetic instability is due to the ability of R loops to stall the progression of the replication fork, leading to its collapse (García-Muse and Aguilera 2016). Thus, RNA–DNA helicases are required for the replication of highly transcribed regions (Boubakri et al. 2010), and R-loop accumulation impairs replication fork progression from bacteria to human cell lines (Wellinger et al. 2006; Tuduri et al. 2009; Gan et al. 2011; Castellano-Pozo et al. 2012; Hamperl et al. 2017). Alternatively, R loops may generate genomic instability if the displaced

[3]**These authors contributed equally to this work.**
Corresponding authors: aguilo@us.es, ana.rondon@cabimer.es
Article published online ahead of print. Article and publication date are online at http://www.genesdev.org/cgi/doi/10.1101/gad.311274.117.

© 2018 García-Rubio et al. This article is distributed exclusively by Cold Spring Harbor Laboratory Press for the first six months after the full-issue publication date (see http://genesdev.cshlp.org/site/misc/terms.xhtml). After six months, it is available under a Creative Commons License (Attribution-NonCommercial 4.0 International), as described at http://creativecommons.org/licenses/by-nc/4.0/.

Downloaded from genesdev.cshlp.org on September 30, 2020 - Published by Cold Spring Harbor Laboratory Press

ssDNA is recognized and processed by flap endonucleases (Sollier et al. 2014). Despite reports showing that R loops alter replication, causing genome instability, the mechanism is still unclear. However, recent evidence indicates that R loops are not deleterious per se but require a second step, such as a local chromatin compaction, to compromise genome integrity (Castellano-Pozo et al. 2012; García-Pichardo et al. 2017).

RNA–DNA hybrids also have a physiological role at telomeres. Telomeres are transcribed into a long non-coding RNA (lncRNA) called TERRA that recruits telomeric proteins, contributes to heterochromatin formation (Maicher et al. 2014), and prevents activation of the DNA damage response (Flynn et al. 2011). A small proportion of TERRA RNA hybridizes with the DNA, forming telomeric RNA–DNA hybrids. This is restrained by the actions of RNase H and the THO complex (Balk et al. 2013; Pfeiffer et al. 2013; Arora et al. 2014; Yu et al. 2014) and favored by telomere shortening. TERRA RNA–DNA hybrids promote homologous recombination (Graf et al. 2017) between telomeric repeats, enabling alternative lengthening of telomeres (ALT), a mechanism used by telomerase-deficient tumor cells to prevent telomere shortening (Balk et al. 2013; Arora et al. 2014; Yu et al. 2014).

A number of transcription and RNA processing factors, such as THO or SRSF1, control cotranscriptional R-loop formation (Santos-Pereira and Aguilera 2015). Yra1 is an RNA-binding protein conserved in metazoans (ALY/REF) that acts as an adaptor for mRNA export factors (Kohler and Hurt 2007). It is cotranscriptionally loaded onto RNA by directly interacting with the C-terminal domain (CTD) of RNA polymerase II (RNAPII) (MacKellar and Greenleaf 2011) or with other mRNP assembly factors (Johnson et al. 2011; Ma et al. 2013; Ren et al. 2017). Interestingly, Yra1 stoichiometry is tightly regulated in the cell via a mechanism relying on Yra1 inhibition of *YRA1* pre-mRNA splicing (Rodríguez-Navarro et al. 2002; Preker and Guthrie 2006; Dong et al. 2007). Thus, removal of the *YRA1* intron from the gene bypasses this autoregulatory circuit, causing Yra1 overexpression with a strong negative impact on mRNA export and cell viability (Rodríguez-Navarro et al. 2002; Preker and Guthrie 2006). Interestingly, we reported recently that high Yra1 intracellular levels alter genome dynamics by accumulating DNA damage and causing transcription-associated spontaneous recombination that is suppressed by RNase H overexpression (Gavaldá et al. 2016).

Aiming to understand how Yra1 overexpression and transcription compromise genome integrity, we demonstrate here that excess Yra1 is recruited to chromatin in an RNA–DNA hybrid-dependent manner, thereby stabilizing R loops and converting them into genome integrity threats. Importantly, an excess of Yra1 increases R-loop-mediated genome instability regardless of transcription–replication orientation. Consistent with the fact that Yra1 also binds to telomeres, where R loops accumulate, we show that Yra1 overexpression causes an increase of RNA–DNA hybrids at telomeres, telomere alterations, and accelerated senescence in telomerase-deficient cells. Our results demonstrate not only that excess of Yra1/ALY binds and stabilizes R loops but that R loops are transiently formed in cells regardless of replication, although they need to be stabilized to compromise genome integrity.

Results

Excess Yra1 binds to chromatin in an RNA–DNA hybrid-dependent manner

Since *YRA1* overexpression increases genomic instability in an RNase H-sensitive manner (Gavaldá et al. 2016), we wondered whether overexpressed Yra1 stabilized naturally formed RNA–DNA hybrids. For this, we analyzed whether localization of overexpressed Yra1 to transcribed genes was dependent on RNA–DNA hybrids. We performed an Yra1 chromatin immunoprecipitation (ChIP) in wild-type cells overexpressing or not overexpressing *YRA1* using an HA-tagged Yra1 protein expressed from either an intron-deficient (HA-YRA1Δi) or an intron-containing (HA-YRA1) version of *YRA1*, respectively (Gavaldá et al. 2016). To determine whether putative Yra1 binding to chromatin was dependent on the presence of RNA–DNA hybrids, we overexpressed RNase H, an enzyme that specifically degrades the RNA moiety of RNA–DNA hybrids. Under *YRA1*-overexpressing conditions, we found a clear increase of Yra1 recruitment to the endogenous *GCN4* and *PDR5* genes previously reported to accumulate RNA–DNA hybrids (García-Benítez et al. 2017) and to the *YRA1* intron region. Overexpressing RNase H in the cell, we restored Yra1 basal levels in all of the regions analyzed (Fig. 1A). These observations argue that Yra1 is recruited to RNA–DNA hybrids when artificially overexpressed in addition to their natural putative RNA.

Yra1 increases RNA–DNA hybrid accumulation in vivo

Next, we determined whether RNA–DNA hybrids were increased, presumably due to stabilization, when *YRA1* was overexpressed. We performed a DNA–RNA immunoprecipitation (DRIP) with the S9.6 antibody in wild-type cells overexpressing (HA-YRA1Δi) or not overexpressing (HA-YRA1) *YRA1* to detect the hybrids. We focused on the genomic regions where we showed a hybrid-dependent Yra1 localization: *GCN4*, *PDR5*, and *YRA1* introns. We observed a S9.6 signal in the three regions analyzed that was significantly reduced by RNase H treatment (Fig. 1B). The RNA–DNA hybrids detected in *GCN4*, *PDR5*, and *YRA1* introns were significantly increased when *YRA1* was overexpressed (Fig. 1B).

Next, we examined whether Yra1 recruitment was enriched at regions naturally forming RNA–DNA hybrids genome-wide when overexpressed. We performed S9.6 DRIP-seq (DRIP combined with high-throughput sequencing) analysis in wild-type cells and compared the data with our previously published ChIP–chip data on Yra1 recruitment (HA-Yra1 and HA-Yra1Δi) (Gavaldá et al. 2016). Our DRIP-seq data are consistent with previously published S9.6 ChIP-seq (ChIP combined with high-

Downloaded from genesdev.cshlp.org on September 30, 2020 - Published by Cold Spring Harbor Laboratory Press

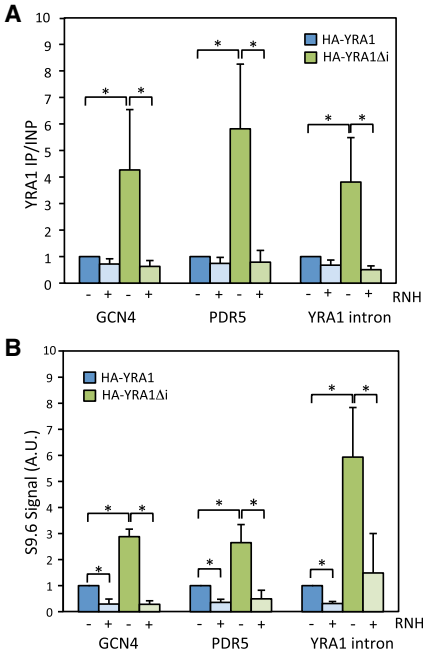

Figure 1. *YRA1* overexpression causes RNA–DNA hybrid accumulation. (*A*) ChIP analysis of Yra1 using anti-HA antibody in a wild-type strain overexpressing (green, HA-YRAΔi) or not overexpressing (blue, HA-YRA1) *YRA1* and RNaseH (RNH$^+$ or RNH$^-$) at the *GCN4* and *PDR5* genes or the *YRA1* intron. $n > 3$. (*B*) DNA–RNA immunoprecipitation (DRIP) with the S9.6 antibody in wild-type asynchronous cultures overexpressing (HA-YRAΔi; green) or not overexpressing (HA-YRA1; blue) *YRA1* at the *GCN4* and *PDR5* genes or the *YRA1* intron. $n > 3$. Samples were treated (+) or not (–) in vitro with RNase H (RNH) prior to the immunoprecipitation. Means and SEM are plotted in all panels. (*) $P < 0.05$, two-tailed Student's *t*-test.

throughput sequencing) data (El Hage et al. 2014), with a significant overlap in the mitochondrial DNA profile and nuclear peaks and genes (Fig. 2A; Supplemental Fig. S1A,B). Comparison with the distribution of Yra1 at wild-type levels (HA-Yra1) or overexpressed (HA-Yra1Δi) revealed a significant correlation between hybrids and Yra1 signals. In our study, the majority of the DRIP signal mapped on ORFs, tRNA genes, and mobile elements, consistent with other reports (El Hage et al. 2014), even though we detected fewer peaks (Supplemental Fig. S1C). Overexpressed Yra1 localized at 1923 genes (Fig. 2B; Supplemental Fig. S1D), with a significant overlap between Yra1-bound genes in cells overexpressing Yra1 and the RNA–DNA hybrid-accumulating genes in wild-type cells (25% or 53% when compared with our new DRIP-seq or the previously published ChIP-seq data) (Fig. 2B; Supplemental Fig. S1D). In summary, the results suggest that overexpressed Yra1 binds to R-loop-accumulating regions genome-wide. Certainly, Yra1 still binds to regions without detectable DRIP signal, as expected from an RNA-binding protein involved in mRNA export.

We finally investigated the effect of Yra1-mediated hybrid stabilization in cell fitness. For this, we overexpressed *YRA1* in mutants that accumulate R loops, such as *hpr1Δ*, *mft1Δ*, or *tho2Δ* mutants lacking the THO complex involved in mRNP biogenesis or the double-mutant *top1Δ top2-1* that accumulates negative supercoiling favoring R loops (Supplemental Fig. S2). As can be seen, the results showing a decrease in cell viability suggest that the increase in persistent RNA–DNA hybrids in *YRA1*-overexpressing cells could contribute to cell death.

An mRNA export defect is not sufficient to increase R loops

Since overexpression of Yra1 impairs mRNA export (Rodríguez-Navarro et al. 2002), we wanted to confirm that the nuclear mRNA accumulation resulting from an mRNA export defect was not sufficient to increase R loops. We analyzed three different nucleoporin mutants (*nup42Δ* and *nup60Δ*, known to be affected in mRNA export, and *nup100Δ*, not affected) (Bonnet and Palancade 2014) and the positive control (*mlp1Δ*, a nuclear pore mutant known to accumulate R loops) (García-Benítez et al. 2017). R loops were inferred using a genetic method based on the hyperrecombination ability of the human activation-induced cytidine deaminase (hAID), an enzyme that modifies cytidines in the ssDNA moiety of the R loop, as shown previously (García-Benítez et al. 2017; García-Pichardo et al. 2017). Recombination in *nup42Δ* and *nup100Δ* was similar to the wild type, whereas in *nup60Δ* it was increased (4.3×), but this increase was not suppressed by RNase H overexpression, consistent with its known sensitivity to HU and MMS (Niño et al. 2016) and in contrast to the positive control *mlp1Δ* (Supplemental Fig. S3). Therefore, we conclude that accumulation of mRNA in the nucleus due to an RNA export defect does not induce R loops per se.

Yra1 binds RNA–DNA hybrids in vitro

Since Yra1 localizes to RNA–DNA hybrid-enriched regions and is a well-characterized RNA-binding protein, we reasoned that Yra1 might directly bind to RNA–DNA hybrids. To test this idea, we isolated a recombinant His_6-tagged version of Yra1 from bacteria, confirming it by Western blot (Supplemental Fig. S4). Next, we performed a gel mobility shift assay incubating increasing amounts of Yra1 with a 25-base-pair (bp) RNA–DNA hybrid that was formed by annealing an RNA oligonucleotide to the complementary radioactively labeled DNA. In parallel, we assayed Yra1 binding to the same radioactive end-labeled RNA or DNA oligonucleotide that forms the hybrid and to a dsRNA constructed by annealing the same end-labeled RNA and a complementary RNA. We observed a shift in RNA migration (confirming the previously described Yra1 ability to bind RNA) but also in ssDNA, dsRNA, and, more importantly, RNA–DNA hybrid migration (Fig. 3A). Since the RNA–DNA hybrid and the ssDNA migrate differently (Fig. 3A, lanes 6,11), we concluded that all labeled ssDNA is present in the form of an RNA–DNA hybrid, as only one band is observed in the sample without Yra1 (Fig. 3A, lane 11).

Downloaded from genesdev.cshlp.org on September 30, 2020 - Published by Cold Spring Harbor Laboratory Press

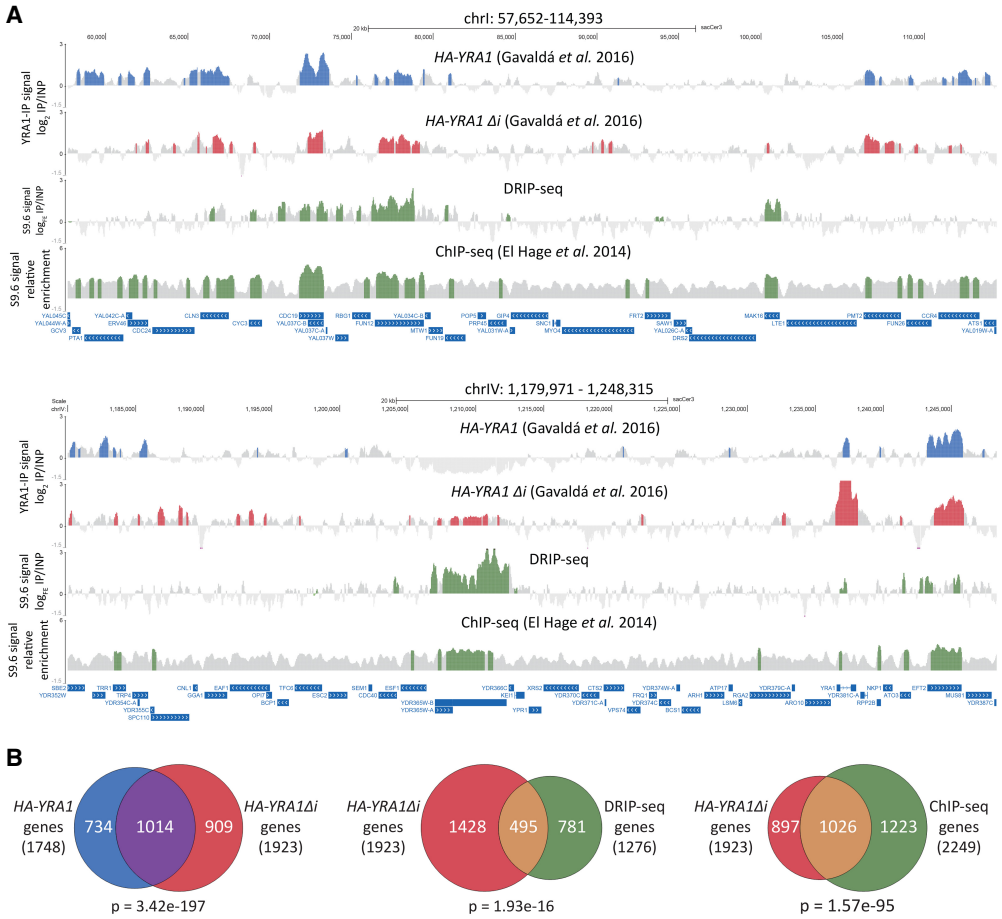

Figure 2. Genome-wide correlation between *YRA1* overexpression and RNA–DNA hybrids. (*A*) Genomic view of Yra1 recruitment in a wild-type strain overexpressing (*HA-YRAΔi*) or not overexpressing (*HA-YRA1*) *YRA1* and RNA–DNA hybrid distribution. Fragments of chromosome I (chr1; *top*) and chromosome IV (chrIV; *bottom*) are plotted with the signal $\log_2$ ratio values of the ChIP–chip from Gavaldá et al. (2016), the $\log_{FE}$ of immunoprecipitation over input for the wild-type (W303) DRIP-seq, and the relative enrichment of reads over the background level of sequencing in a wild-type strain (El Hage et al. 2014). Blue (HA-YRA1 IP), red (HA-YRA1Δi), and green (DRIP-seq or ChIP-seq) histograms represent the significant clusters. SGD features are represented *below* as blue bars. Profiles were represented using the University of California at Santa Cruz Genome Browser. (*B*) Venn diagrams showing the overlap between gene sets with significant Yra1 binding in the different ChIP–chip experiments from Gavaldá et al. (2016) (HA-YRA1 IP [blue] and HA-YRA1Δi [red]) and significant RNA–DNA hybrid accumulation (DRIP-seq from this study or ChIP-seq from El Hage et al. [2014]; green). *P*(*x*) was calculated with the hypergeometric distribution formula.

Therefore, Yra1 is able to bind in vitro not only ssRNA but also ssDNA, dsRNA, and a RNA–DNA duplex. To confirm these interactions, we competed Yra1 binding with different cold nucleic acid species. First, we incubated purified Yra1 with labeled dsRNA and increasing amounts of cold ssRNA or RNA–DNA hybrid. Both nucleic acids reverted Yra1 interaction with dsRNA at similar concentrations (5 µM) (Fig. 3B). Next, we challenged the Yra1–hybrid interaction with increasing amounts of cold hybrid, ssRNA, or ssDNA. In agreement with its binding to RNA–DNA hybrids, cold ssRNA, ssDNA, or RNA–DNA hybrids competed for Yra1 binding, since RNA–DNA hybrids are slightly better competitors than ssRNA and ssDNA (Fig. 3C). Altogether, these results indicate that Yra1 is able to bind RNA–DNA hybrids, supporting the conclusion that when overexpressed in vivo, Yra1 can bind R loops in chromatin, contributing to their stabilization.

R-loop-mediated genome instability is linked to head-on transcription–replication

We showed previously that transcription causes hyperrecombination when occurring in a head-on orientation with respect to replication but not when occurring codirectionally (Prado and Aguilera 2005). Since RNA–DNA hybrids are an obstacle for replication fork progression (Wellinger et al. 2006; Gan et al. 2011), we examined whether they could explain the orientation-dependent transcription–replication conflicts responsible for genome instability. We used the previously reported plasmids pGAL-OUT and pGAL-IN (Prado and Aguilera

Downloaded from genesdev.cshlp.org on September 30, 2020 - Published by Cold Spring Harbor Laboratory Press

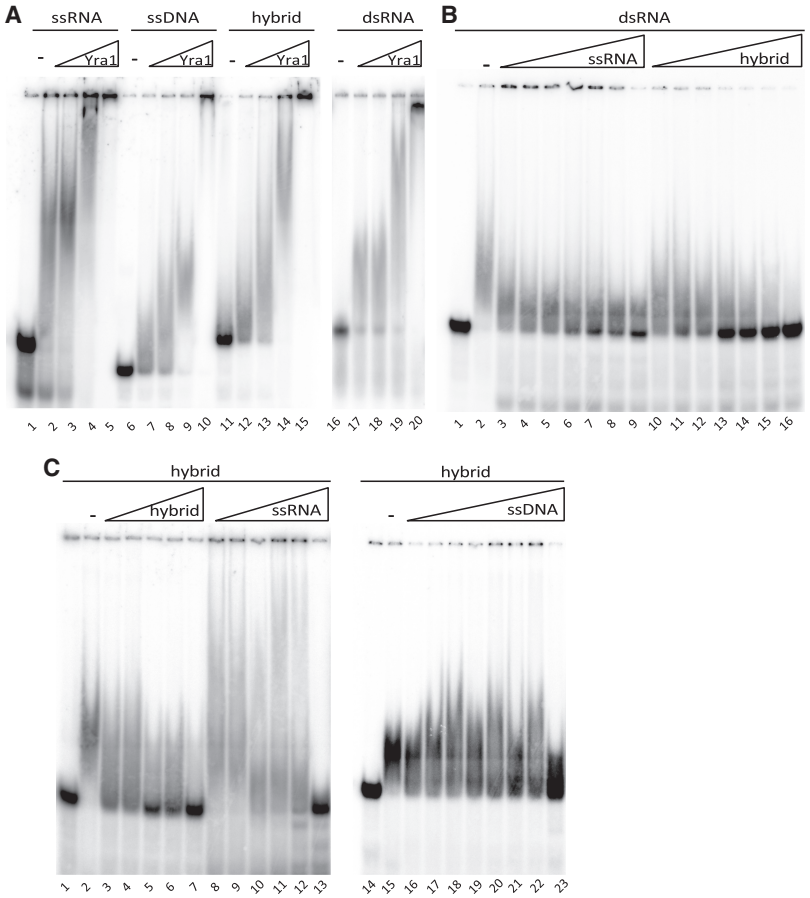

Figure 3. *YRA1* binds to RNA–DNA hybrids in vitro. (*A*) Electrophoretic mobility shift assay (EMSA) of His_6-Yra1 and either ssRNA, ssDNA, or RNA–DNA hybrids formed by annealing the ssRNA and ssDNA probes used in the single experiments or dsRNA. (*B*) EMSA of His_6-Yra1 and dsRNA competed with increasing amounts of cold ssRNA or RNA–DNA hybrids (0.6–40 µM). (*C*) EMSA of His_6-Yra1 and RNA–DNA hybrids competed with increasing amounts of cold RNA–DNA hybrids (0.25–8 µM) or ssRNA or ssDNA (0.25–16 µM).

2005) that contain *leu2* truncated repeats transcribed from an inducible *GAL1* promoter in either a codirectional (OUT) or head-on (IN) orientation with respect to replication driven from the early replication origin *ARSH4* (Fig. 4A), respectively. DNA damage driven by the transcription–replication collision would be repaired by recombination between the *leu2* direct repeats, generating a wild-type *LEU2* gene. Consequently, we could measure genome instability as the frequency of $Leu2^+$ recombinant colonies. We observed that the frequency of recombination in the absence of transcription was low and similar in both systems (Fig. 4B), consistent with previous results (Prado and Aguilera 2005). However, upon transcription, induction recombination was highly increased (7.7-fold) in the IN system with head-on transcription–replication, whereas only a twofold increase in recombination was observed in the codirectional OUT system (Fig. 4B). When similar experiments were performed in both systems after RNase H overexpression, the transcription-dependent hyperrecombination observed in the head-on IN system was suppressed, whereas the recombination frequencies in the codirectional OUT system did not change (Fig. 4B). These results argue that RNA–DNA hybrids are an important source of genome instability in systems undergoing head-on transcription–replication conflicts but not in those undergoing codirectional conflicts. This interpretation would be consistent with the recent observation in human cells using similarly designed plasmid-based constructs in which transcription is driven from a bacterial T7 promoter and replication is driven from an Epstein-Barr virus replication origin (Hamperl et al. 2017) as well with R-loop-dependent replication impairment observed in the *Bacillus subtillis* genome (Lang et al. 2017). However, none of these results provide any answer to whether R loops are formed only in head-on transcription–replication or after replication.

Yra1-stabilized R loops induce instability regardless of transcription–replication orientation

If Yra1 binds and stabilizes transient RNA–DNA hybrids present in the genome, we might expect that Yra1 will increase transcription–replication conflicts mediated by these structures. To test this hypothesis, we measured recombination in the codirectional and head-on systems either overexpressing (YRA1Δi) or not overexpressing (YRA1) *YRA1*. Yra1 overexpression enhanced recombination 7.2 times in the head-on IN system, an increase that was majorly suppressed by RNase H overexpression (Fig. 4C). Importantly, an 8.7-fold increase was also observed in the codirectional OUT system, which was also suppressed by RNase H (Fig. 4C). This result indicates that RNA–DNA hybrids also form under codirectional transcription–replication, but such hybrids are not stable

Downloaded from genesdev.cshlp.org on September 30, 2020 - Published by Cold Spring Harbor Laboratory Press

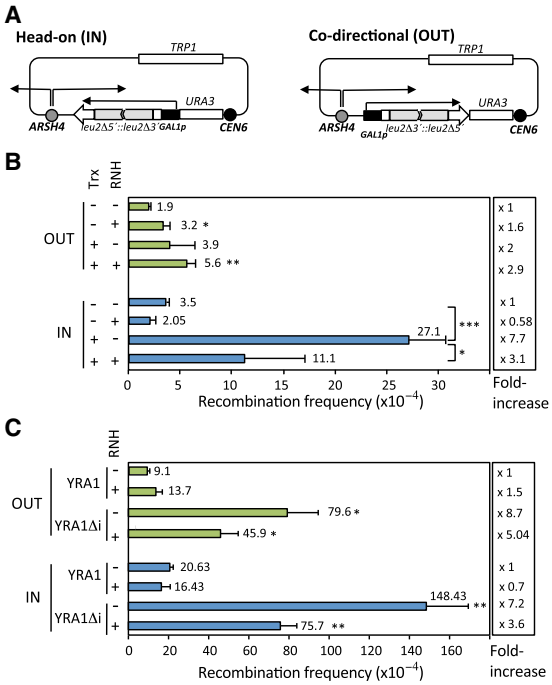

Figure 4. R-loop-mediated transcription–replication conflicts are orientation-independent in *YRA1*-overexpressing cells. (*A*) Schemes of the centromeric plasmids harboring the recombination systems in head-on (IN) and codirectional (OUT) orientation. The arrows indicate the RNAPII-driven transcription orientation of the *leu2* repeats from the *GAL1* promoter and the direction of replication forks initiated at *ARSH4*. (*B*) The effect of RNaseH1 overexpression on the recombination of the head-on (IN) and codirectional (OUT) systems in wild-type cells. Cells grown in either glucose (TRX^-) or galactose (TRX^+) and overexpressing (RNH^+) or not overexpressing (RNH^-) RNase H. The fold increase over no transcription and no RNase H expression is indicated at the *right*. (*C*) The effect of RNH1 overexpression on the recombination of transcribed IN or OUT plasmids in wild-type cells overexpressing (*YRA1Δi*) or not overexpressing (*YRA1*) *YRA1* and RNase H (RNH^+ or RNH^-). The fold increase over no overexpression of *YRA1* and Rnase H is indicated at the *right*. Means and SEM are plotted in all panels. Asterisks indicate statistically significant differences between the strains indicated, according to Student's *t*-tests. (*) $P < 0.05$; (**) $P < 0.005$; (***) $P < 0.0005$.

enough to drive high genome instability. However, under Yra1 overexpression, hybrids are stabilized, resulting in a significant increase in recombination, presumably by constituting a stable block to replication fork progression regardless of transcription–replication orientation.

Therefore, our hypothesis predicts that RNA–DNA hybrids should be present in both plasmids. Consequently, we performed a DRIP analysis using the S9.6 antibody in samples with or without RNase H treatment. In the analysis, we included the previously described hybrid-accumulating *PDR5* gene as an internal positive control and *PRE1* as a negative control. The results confirmed the presence of RNA–DNA hybrids in the plasmid-borne *LEU2* gene of the recombined head-on IN system, in agreement with the in vivo data (Fig. 5A). Notably, we also detected hybrids in the recombined OUT system where *LEU2* transcription is codirectional to replication fork progression (Fig. 5A). Therefore, we conclude that RNA–DNA hybrids are formed during transcription in both codirectional and head-on constructs but significantly induce genomic instability, measured as recombination, when replication and transcription are head-on and not when they are codirectional. However, when the hybrid is stabilized via binding to Yra1, replication would stall regardless of the transcription orientation, leading to a similar increase in recombination (sevenfold to eightfold above the wild-type levels). These results clearly support that R loops are formed transiently regardless of replication and not as a consequence of transcription–replication conflicts.

Although unlikely, it might be possible that circular plasmids impose a specific topological constraint different from chromosomes that could enhance R-loop accumulation and Yra1 binding. To confirm that this was not the case and that R loops occurred in linear chromosomes, we constructed a transcription–replication collision system in chromosome III and analyzed RNA–DNA hybrids under the same conditions tested in the plasmid construct. To do so, we integrated the *LEU2* gene under the inducible *GAL1* promoter in a head-on orientation with respect to replication driven from the early-firing *ARS315* origin (Fig. 5B), since this orientation was the one with the potential to cause DNA opening that could favor R loops. DRIP analyses of cells cultured in galactose-containing medium (transcription ON) versus glucose-containing medium (transcription off) revealed that RNA–DNA hybrids appeared in the *LEU2* gene only when transcribed (Fig. 5B). In the *PDR5* gene used as a positive control, hybrids were observed in both conditions, consistent with the fact that *PDR5* is constitutively transcribed in both media (Fig. 5B). Importantly, the RNA–DNA hybrids formed in the chromosomal transcription–replication collision system increased when *YRA1* was overexpressed (Fig. 5B), in agreement with the increase in recombination observed in the plasmid (Fig. 4C).

Cumulative evidence with concomitant studies on RNA–DNA hybrids, γH2AX, and 53BP1 foci and recombination, comet, and DNA-combing assays suggests that R-loop-dependent γH2AX is the result of DNA damage (García-Rubio et al. 2015; Schwab et al. 2015; Salas-Armenteros et al. 2017). To assess whether the RNA–DNA hybrids detected in the *LEU2* gene cause DNA damage, we measured H2A-P (the equivalent in yeast to γH2AX) levels by ChIP under conditions of both active and inactive transcription of the *GAL1::LEU2* fusion, using telomeric repeats as a positive control (Kitada et al. 2011). An increase in H2A-P was observed when transcription of *LEU2* was active, but not when it was inactive, as well as in the telomeric controls (Fig. 5C). Therefore, head-on transcription of the chromosomal *LEU2* gene also generates DNA breaks. Notably, such breaks were suppressed by RNase H overexpression (Fig. 5C), confirming that they were R-loop-dependent. Most important, such H2A-P foci were significantly increased when Yra1 was overexpressed, and this increase was suppressed by

Downloaded from genesdev.cshlp.org on September 30, 2020 - Published by Cold Spring Harbor Laboratory Press

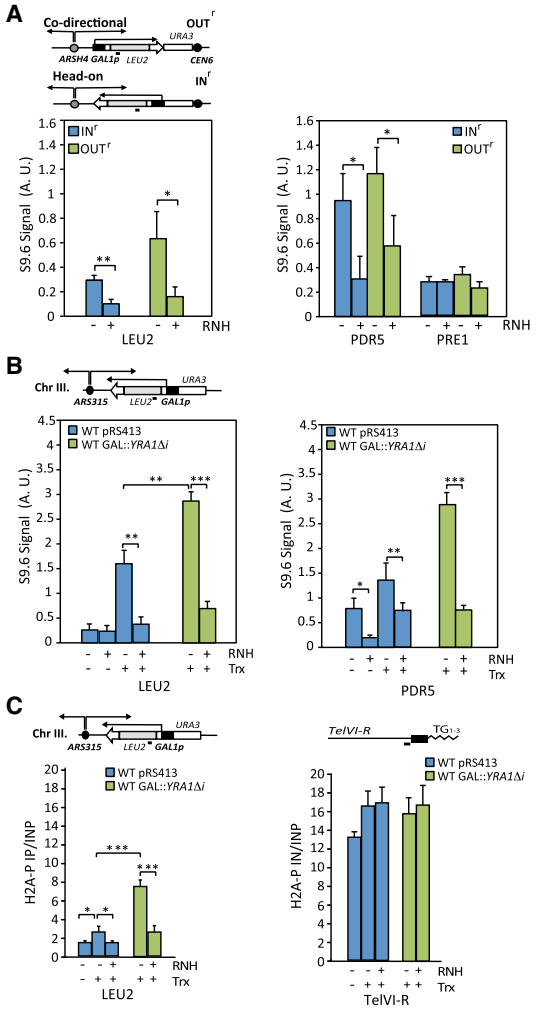

Figure 5. Effect of Yra1 overexpression on transcription–replication collision-mediated genome instability. (*A*) DRIP with the S9.6 antibody in a wild-type strain carrying the recombined head-on (IN^r) and codirectional (OUT^r) plasmid. Samples from asynchronous cultures grown in galactose were treated (+) or not (−) in vitro with RNase H (RNH). The regions assayed were the *LEU2* gene of the plasmid and the chromosomal *PDR5* and *PRE1* (negative control) genes. $n > 3$. (*B*) DRIP assay in wild-type strain with the *GAL1::LEU2* (*URA3*) system integrated in chromosome III (Chr III) close to *ARS315* in head-on orientation. Nucleic acids from cells grown in either glucose (Trx^-) or galactose (Trx^+) were treated with RNase H (RNH^+) prior to the immunoprecipitation with S9.6 antibody. Samples from cells grown in galactose (Trx^+)-overexpressing (GAL::YRA1Δi) *YRA1* are shown in green. The regions assayed were the *LEU2* gene at the head-on OUT^r integrated system and the chromosomal *PDR5* gene. $n > 3$. (*C*) ChIP analysis of H2A-P in the *GAL1::LEU2* (*URA3*) construct integrated in chromosome III (Chr III) in head-on orientation with respect to replication. Cells transformed with *GAL1::RNH1* (RNH^+) or with the empty vector (RNH^-) were grown in glucose (Trx^-) or galactose (Trx^+). $n > 3$. Cells overexpressing (GAL::YRA1Δi) *YRA1* are shown in green. The regions assayed were the *LEU2* gene at the head-on IN^r integrated system and the telomere (*TELVI-R*). $n > 3$. Means and SEM are plotted in all panels. Asterisks indicate statistically significant differences between the strains indicated, according to Student's *t*-tests. (*) $P < 0.05$; (**) $P < 0.005$; (***) $P < 0.0005$.

RNH1 overexpression. The results, in addition to validating our studies in plasmid-borne constructs, indicate that the genomic instability derived from transcription–replication collisions is mediated by RNA–DNA hybrids and not by any specific topological constraints that could potentially accumulate in circular plasmids and that the negative impact of those collisions is enhanced by Yra1 overexpression.

An excess of Yra1 produces telomere shortening and premature senescence in telomerase-deficient cells

We showed recently that an excess of Yra1 causes a cell senescence-like phenotype and a slight telomere shortening in telomerase-positive cells and is enriched at Y′ telomeric regions (Gavaldá et al. 2016). Since Yra1 is a highly efficient RNA-binding protein (Fig. 3; Strasser and Hurt 2000) and since telomerase activity in wild-type cells relies on an RNA molecule that is used as a template for telomere synthesis, it was possible that an excess of Yra1 sequestered the telomerase RNA molecule TLC1, leading to a telomerase-deficient phenotype instead of acting directly on the telomere. To test this possibility, we determined the effects of Yra1 overexpression in telomerase-minus cells (*est2Δ*). Heterozygous *EST2/est2Δ* diploids harboring the *pGAL::Yra1Δi* plasmid were sporulated in glucose medium. Next, haploid *est2Δ pGAL::Yra1Δi* spore clones were selected in glucose medium and further propagated in galactose liquid medium via serial dilutions (Hardy et al. 2014). The senescence profiles, kinetics of telomere shortening, and the type of survivors formed in multiple *est2Δ* and *est2Δ pGAL::Yra1Δi* clones grown in galactose were analyzed (Fig. 6). We showed that *est2Δ pGAL::Yra1Δi* clones (overexpressing Yra1) exhibited a rapid and deep premature senescence compared with *est2Δ* clones (Fig. 6A). Strikingly, telomere length analysis at the first time point of the senescence assay indicated that telomeres were shorter in the *est2Δ pGAL::Yra1Δi* clones compared with *est2Δ* clones (Fig. 6B–D). This result suggests an abrupt telomere shortening upon overexpression of Yra1 different from the progressive telomere erosion normally observed in the absence of telomerase. Consistently, survivors appeared earlier in *est2Δ* cells overexpressing *YRA1* (Fig. 6C). As predicted, RNA–DNA hybrids were increased in *est2Δ* cells (Fig. 6E) as shown in the single *TelVI-R* telomere and consistent with previous results indicating that shortening of telomeres in *est2Δ* cells triggers TERRA transcription and RNA–DNA hybrid accumulation (Graf et al. 2017). Importantly, such hybrids were significantly increased under Yra1 overexpression, consistent with a putative role of Yra1 overexpression in RNA–DNA hybrid stabilization (Fig. 6E).

As expected, in *est2Δ* cells after the onset of senescence, the liquid culture was dominated mainly by type II survivors because of their growth advantage over type I survivors. In contrast, *est2Δ pGAL::Yra1Δi* cultures appeared to produce few type II survivors and a higher proportion of type I survivors. Quantification of the occurrence of type II recombination events at a single telomere, *TELVI-R*, further confirmed that overexpression of *YRA1* impairs

Downloaded from genesdev.cshlp.org on September 30, 2020 - Published by Cold Spring Harbor Laboratory Press

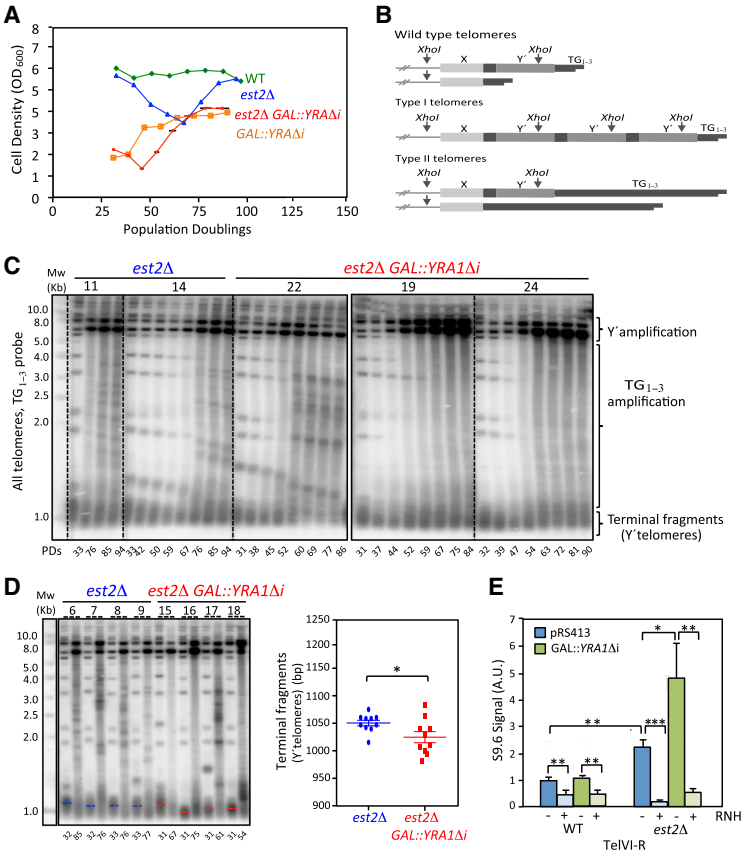

Figure 6. Premature senescence and accelerated shortening of telomeres promoted by Yra1 overexpression. (*A*) Mean growth curves over time of wild type ($n = 2$), GAL::*Yra1Δi* ($n = 2$), *est2Δ* ($n = 10$), and *est2Δ* GAL::*Yra1Δi* ($n = 10$). Each clone corresponds to a spore isolated from the heterozygous diploid strain, propagated in liquid culture through daily serial dilutions every 2 d. OD_{600} was measured every 2 d to estimate the cell density. Population doublings (PDs) were estimated from the initial spores. (*B*, *top*) Schematic representation of wild-type, type I, and type II telomeres. All telomeres contain one X element in the subtelomeric region and from zero to four long (L) or short (S) Y′ subtelomeric sequences. Type I survivors show an amplification of Y′ sequence and interstitial $TG_{1–3}$ repeats. Type II survivors display an elongation of $TG_{1–3}$ terminal repeats. Positions of the XhoI sites are shown. (*C*) $TG_{1–3}$-probed Southern blot analysis of the telomere length of representative clones of *est2Δ* and *est2Δ* GAL::*Yra1Δi* during senescence. (*D*) Southern blot analysis and mean telomere length at the first time point. $n = 10$. (*E*) DRIP with the S9.6 antibody in wild-type and *est2Δ* strains. Nucleic acids were treated with RNase H (RNH^+) prior to the immunoprecipitation with S9.6 antibody. Samples from cells grown in galactose (Trx^+)-overexpressing (GAL::YRA1Δi) *YRA1* are shown in green. The region assayed was the telomere (*TELVI-R*). $n > 3$. Means and SEM are plotted in all panels. Asterisks indicate statistically significant differences between the samples indicated, according to Student's *t*-tests. (*) $P < 0.05$; (**) $P < 0.005$; (***) $P < 0.0005$.

type II recombination (Fig. 7). These results unequivocally indicate that it is the high accumulation of overexpressed Yra1 at telomeres (Gavaldá et al. 2016) rather than an inhibition of telomerase activity due to the sequestering of the RNA template that causes a quick and profound shortening of telomeres and premature senescence. We also noticed an increase of Y′ amplification upon Yra1 overexpression, although this increase did not reach a statistical significance (Supplemental Fig. S5).

Finally, we tried to determine the impact of RNH1 overexpression on senescence and telomere dynamics in *est2Δ* cells overexpressing Yra1. However, RNase H overexpression leads to a very sick phenotype of telomerase-deficient *est2Δ* cells overexpressing Yra1 (Supplemental Fig. S6). These cells entered crisis quickly with a very low viability compared with *est2Δ* cells overexpressing only Yra1. Unfortunately, it is not possible to know whether this behavior is the result of two independent types of stresses (RNase H and Yra1 overexpression) or whether the two processes are interdependent, and any interpretation about the type of survivors was hampered by the very low cell density at crisis in cells co-overexpressing Rnh1 and Yra1. Indeed, since survivors result from clonal events, the large heterogeneity might simply reflect differences among their very low cell densities. Therefore, we cannot conclude whether RNase H overexpression counteracts Yra1 overexpression or potentiates its effect on telomere dynamics, both possibilities being consistent in any case with the increased presence of RNA–DNA hybrids at telomeres (Fig. 6E).

Discussion

After demonstrating that the RNA-binding factor Yra1 can bind RNA–DNA hybrids in vitro and in vivo, we showed that dynamic DNA–RNA hybrids are bound by overexpressed Yra1 and threaten genome integrity by promoting transcription–replication collisions. This is a general effect occurring all over the genome. Hyperrecombination caused by transcription–replication collisions is R-loop-dependent and specific to head-on orientation, not being observed for codirectional transcription. Importantly, overexpression of Yra1 causes a similar and significant sevenfold to eightfold increase in R-loop-dependent recombination in systems undergoing either head-on or codirectional transcription–replication collisions. This suggests that RNA–DNA hybrids are cotranscriptionally formed independently of replication, but only when the replication fork approaches an R loop from downstream from the RNAP does it compromise genome integrity. Thus, the replication fork progressing in the same direction as transcription may easily resolve an R loop, unless Yra1 is bound to it. The ability of Yra1 to bind R loops and block replication dynamics is supported by the fact that Yra1 overexpression shortens telomeres by a telomerase-

Downloaded from genesdev.cshlp.org on September 30, 2020 - Published by Cold Spring Harbor Laboratory Press

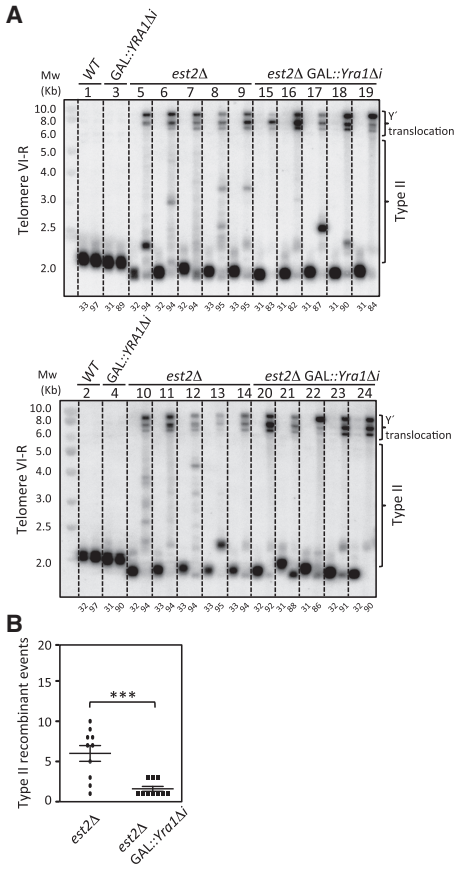

Figure 7. Analysis of type II recombination events at *TELVI-R*. (*A*) The clones used in Figure 6 were analyzed by single-telomere Southern blot at the first time point of senescence and after the appearance of survivors. Each band corresponds to a single type II recombination event in the cell population independently of its intensity. (*B*) The frequency of type II recombination events at *TELVI-R*. Details are as in Figure 6D.

independent mechanism presumably linked to R loops generated by TERRA RNA, which is yet to be understood. These data indicate that R loops form transiently in the cell regardless of replication and generate genome instability mainly in head-on orientation or when they are stabilized by proteins such as Yra1 by impeding the progression of replication.

We showed here that the Yra1 RNA-binding factor can bind and presumably stabilize RNA–DNA hybrids in vitro and in vivo when overexpressed, although this would not be its role when present at wild-type levels in the cell. Interestingly, *Arabidopsis* AtNDX, a homeodomain-containing protein, stabilizes R loops by binding to the displaced ssDNA (Sun et al. 2013). In contrast to AtNDX, Yra1 is an RNA-binding protein that presumably affects R-loop dynamics by binding to the RNA–DNA hybrids, likely impeding the action of helicases and RNase H and leading to the accumulation of stable or more persistent R loops. Indeed, Yra1 inhibits loading of Dbp2, an RNA helicase with in vitro RNA–DNA-unwinding activity (Ma et al. 2013, 2016). However, the in vitro ssDNA-binding ability observed for Yra1 (Fig. 3) suggests that Yra1 would also bind the displaced ssDNA of the R loops, potentially strengthening the stabilization and lengthening the persistency of the three-stranded R-loop structure in vivo. Although Yra1 overexpression impairs mRNA export (Rodríguez-Navarro et al. 2002), we showed that a defect in mRNA export is not sufficient to produce either R-loop accumulation or R-loop-dependent hyperrecombination (Supplemental Fig. S3) and that Yra1 binding to transient RNA–DNA hybrids and other RNA structures may also contribute to its deleterious effect (Supplemental Fig. S2). Indeed, RNase H expression reduces not only recombination and DNA damage but also recruitment of Yra1 to chromatin at transcribed genes (Fig. 1A). Thus, the ability of Yra1, in cells overexpressing it, to bind and fix R loops and compromise genome integrity might explain, at least in part, its specific regulation to avoid its overexpression.

How transcription induces genome instability is not fully understood yet, but research conducted in the last two decades points to conflicts with replication as a major source of transcription-associated instability (García-Rubio et al. 2003; Prado and Aguilera 2005; Mirkin and Mirkin 2007; Boubakri et al. 2010). The transcription-dependent recombination results obtained in the codirectional and head-on systems when Yra1 is overexpressed reveal that R loops are a key player in transcription–replication conflicts (Fig. 4C). This is in agreement with previous work showing that R-loop-accumulating mutants hinder replication in yeast, *Caenorhabditis elegans*, or human cell lines (Wellinger et al. 2006; Gan et al. 2011; Castellano-Pozo et al. 2012) and that, in bacteria, the RNA–DNA helicase *DinG* is essential for replication of highly transcribed regions (Boubakri et al. 2010). Interestingly, we showed that R loops by themselves may not be strong inducers of genome instability; instead, they rely on a subsequent step to compromise genome integrity (García-Pichardo et al. 2017). One such step is linked to the modification of chromatin via histone H3 Ser10 phosphorylation (H3S10-P), a mark of chromatin condensation, which reveals that a local chromatin compaction triggered by an R loop may be behind its negative impact on replication progression and genome integrity (Castellano-Pozo et al. 2012; García-Pichardo et al. 2017). Thus, naturally formed R loops are presumably transient, with no consequence on genome integrity. However, here we demonstrate that by artificially stabilizing transient R loops by binding to overexpressed Yra1, R loops accumulate at high levels and compromise genome integrity.

We showed previously that transcription induces hyperrecombination only when it occurs concomitantly with replication and in head-on orientation (Prado and Aguilera 2005). Now we show that the hyperrecombination induced in the head-on orientation is largely dependent on R loops (Fig. 4) but not codirectional collisions. These results are consistent with two recent reports in bacteria and human cells showing that codirectional transcription–replication conflicts have little impact on the stability of the construct-containing plasmid or on bacteria viability, while head-on orientation is unstable and causes

Downloaded from genesdev.cshlp.org on September 30, 2020 - Published by Cold Spring Harbor Laboratory Press

lethality in RNase H-deficient bacteria (Hamperl et al. 2017; Lang et al. 2017). Nevertheless, the S9.6 DRIP analysis reveals that RNA–DNA hybrids are formed in *LEU2* in not only the head-on but also the codirectional system, although they do not largely compromise the genome integrity. We detected R loops regardless of transcription–replication orientation, but when Yra1 is overexpressed, an R-loop-dependent increase in recombination occurred in both systems, whether head-on or codirectional, demonstrating that they are present in both situations. Therefore, our data indicate that R loops are formed cotranscriptionally regardless of replication and may be present before the replication fork arrives; that is, it is not the transcription–replication collisions the cause of the R loops (Bermejo et al. 2011; Hamperl et al. 2017; Lang et al. 2017). Consistently, R loops are also observed in the codirectional orientation in a bacterial chromosome too (Lang et al. 2017) and are detected in G1 cells in yeast and human cells (Castellano-Pozo et al. 2012; Bhatia et al. 2014). Therefore, we conclude that R loops are the cause and not the consequence of transcription–replication collisions, consistent with the genome-wide accumulation of RNA–DNA hybrids detected in our study (Fig. 2; Supplemental Fig. S1) or other previously published reports (Chan et al. 2014; El Hage et al. 2014; Wahba et al. 2016).

We propose that the different outcome of a replisome encountering an R loop codirectionally or head-on may depend on the structure encountered. In codirectional orientation, the replisome would meet the RNA–DNA hybrid directly in the leading strand template, presumably being able to remove it easily with the help of some helicase function (Fig. 8A). However, in the head-on orientation, the fork would encounter first the RNAP that thus would be trapped ahead of the nascent RNA forming the RNA–DNA hybrid in the lagging strand template. In this orientation, the RNAP would be a major contributor to the stalling of the replisome, presumably incapable of backtracking due to the hybrid behind (Fig. 8A). Indeed, it has been shown in bacteria that backtracked RNAP unable to resume transcription would cause DNA breaks when encountered by a replication fork (Nudler 2012). It is worth noting that a physical contact between the replisome and the RNAP might not be necessary, as the positive topological constraint generated in between the two advancing polymerases may be sufficient to block both processes. However, if the R loop is blocked artificially by binding with Yra1 when it is in excess in the cell, then it becomes an obstacle to replication no matter from which direction it is encountered (Fig. 8B).

The importance of R-loop stabilization becoming a general obstacle to replication is supported by the analysis of the impact of Yra1 on telomere dynamics and homeostasis, where R loops have been shown to play a role. We show here that Yra1 overexpression causes a telomere-shortening phenotype that is not explained by a potential ability of overexpressed Yra1 to sequester the telomerase TLC RNA. Telomeres are overshortened in the absence of telomerase when Yra1 is overexpressed (Fig. 6), favoring the idea that Yra1 excess would be shortening the telomere through R-loop stabilization. Telomere repeats and subtelomeric regions are transcribed in lncRNAs known as TERRA, which form unstable R loops (Maicher et al. 2014; Azzalin and Lingner 2015) that need to be removed before chromosomal ends are replicated (Graf et al. 2017). Therefore, it is likely that, by stabilizing TERRA R loops, Yra1 overexpression impairs telomere replication progression. Consistent with this idea, overexpressed Yra1 is recruited to telomeres, and Rrm3, the replicative helicase that resolves replication fork stalls, accumulates at telomeres in this situation (Gavaldá et al. 2016). Importantly, the presence of RNA–DNA hybrids at telomeres is higher in *est2Δ* cells, as expected, and significantly enhanced under Yra1 overexpression (Fig. 6E). Fork collapse mediated by stable R loops might be responsible of the telomere shortening, thus causing premature senescence (Simon et al. 2016). Indeed, deletion of RNase H or the THO complex in cells unable to undergo recombination (*rad52Δ*) increases TERRA R loops and leads to rapid telomere loss and senescence (Balk et al. 2013). We observed a reduced appearance of type II telomeres and slightly higher Y′ subtelomeric amplification in the survivors after senescence. This suggests that Yra1 overexpression may favor type I recombination between subtelomeric Y′ elements at the expense of type II recombination. This is consistent with the observation that RNA–DNA hybrids formed by

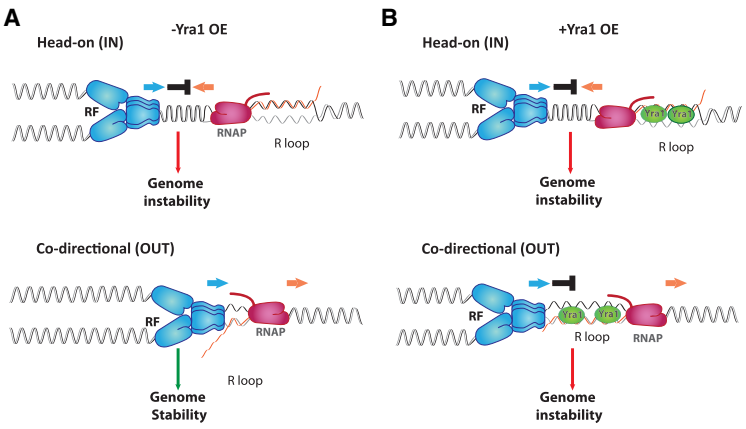

Figure 8. Model to explain Yra1-mediated transcription–replication collisions. (*A*) In the codirectional orientation, the replication fork (RF) encounters the R loop, removing it. In the head-on orientation, either the positive supercoiling accumulated ahead or the RNAP itself would block the replication fork. (*B*) Overexpressed Yra1 (+Yra1 OE) binds to the R loop, stabilizing it and blocking replication whether it proceeds codirectionally or in head-on orientation.

Downloaded from genesdev.cshlp.org on September 30, 2020 - Published by Cold Spring Harbor Laboratory Press

TERRA hybridization at telomeres promote the recruitment of Rad51 (Graf et al. 2017). Collectively, these data support our model that Yra1 binding to R loops causes replication impairment and hyperrecombination all over the genome. The fact that simultaneous overexpression of RNase H and Yra1 makes telomerase-deficient cells extremely sick, triggering a quick entry into crisis, suggests an involvement of RNA–DNA hybrids in this behavior, but we cannot predict whether RNase H overexpression should either counteract or strengthen the impact of Yra1 overexpression on telomere dynamics and senescence without further mechanistic understanding (Supplemental Fig. S6).

In conclusion, we uncovered the role of RNA–DNA hybrids in transcription–replication conflicts regardless of the orientation, indicating that R-loop formation is independent of replication. Artificially stabilized RNA–DNA hybrids cause genome instability when encountered by the replication fork in both head-on and codirectional orientation; otherwise, only RNA–DNA hybrids involved in head-on transcription–replication collisions have a major effect on genome instability. These findings may help understand the role in preventing R-loop accumulation and R-loop-mediated genome instability of specific functions such as histone deacetylase Sin3A, the THO complex, or the Fanconi anemia pathway, which have been shown to impair replication fork progression through R loops when mutated (García-Rubio et al. 2015; Schwab et al. 2015; Madireddy et al. 2016; Salas-Armenteros et al. 2017). Similarly, these results raise the question of whether overabundance of the Yra1 ortholog ALY protein in a significant proportion of tumoral cells may be related to high levels of stabilized RNA–DNA hybrids that contribute to genome instability (Dominguez-Sanchez et al. 2011). This work thus should open new perspectives to understand the mechanisms of R-loop-mediated genome instability and its implications in cancer development.

Materials and methods

Strains, primers, and plasmids

Yeast strains, primers, and plasmids used are listed in Supplemental Tables S1–S3, respectively. The BGL2 strain was generated by integrating in BY4741 the *GAL1::LEU2* (*URA3*) construct at position 225,807 of chromosome III in a head-on orientation relative to replication starting at ARS315. This strain was crossed with Ybp250 to generate BYGL2-10B.

The recombined plasmid pARSGLBIN-Leu2 was used as a template to amplify the *GAL1::LEU2* (*URA3*) construct, adding the BglII restriction site and 40-bp of homology to the region upstream of or downstream from position 225,807 of chromosome III at both sides. The linear PCR fragment was purified and transformed in the BY4741 strain. Ura^+ transformants were checked for *GAL1::LEU2* (*URA3*) integration by Southern blot.

Genome-wide experiments

DRIP was performed as described (García-Pichardo et al. 2017). For sequencing, immunoprecipitation and input samples were used as templates with a GenomePlex Complete whole-genome amplification kit (Merck) to amplify the DNA. The library was prepared to obtain a fragment size of 200 bp according to the manufacturer's protocol (Ion Torrent PGM). The quality of the samples was certified with a Bionalyzer and a high-sensitivity DNA analysis kit, and runs were performed in an Ion 316 ChIP version 2. The data generated are available under Gene Expression Omnibus accession number GSE113580. Bioinformatic analysis was performed as described (see the Supplemental Material). DRIP-seq signal values were multiplied by three for visualization.

Yra1 expression and purification

His_6-tagged Yra1 was expressed from pET-Yra1 (MacKellar and Greenleaf 2011) in BL21 Rossetta *Escherichia coli* (DE3) cells (Novagen). Bacteria were grown in 1 L of LB medium with ampicillin and chloramphenicol, and protein expression was induced with 0.2 mM IPTG overnight at 16°C. Cells were lysed and His_6-Yra1 purified through Ni-Sepharose Fast Flow resin (GE Healthcare) as described (MacKellar and Greenleaf 2011) followed by SP-Sepharose (GE Healthcare) (Ma et al. 2013).

Electrophoretic mobility shift assay

RNA and DNA oligonucleotides purchased from Integrated DNA Technologies (IDT) were end-labeled with ^{32}PATP using T4 polynucleotide kinase according to the manufacturer's instructions. The same nucleic acids were used as cold competitors and added at the concentration indicated. The binding reactions were performed with the indicated nucleic acids at 30–50 nM final concentration and increasing amounts of recombinant Yra1 (170 nM to 1.4 mM) in binding buffer (10 mM Tris-HCl at pH 7.5, 25 mM NaCl, 1 mM DTT, 10% glycerol) supplemented with 0.05 mg/mL BSA, 1× cocktail protease inhibitors, and RNase OUT for 10 min at 30°C. Samples were resolved in 6% PAGE and 0.5× TBE run for 1 h at 15 mA. Gels were dried, and images were taken with a Fujifilm Life Science FLA-5100 imaging system.

DRIP assays

DRIP in *est2Δ* strains was performed as described (García-Rubio et al. 2018) in haploid spore products of diploid PAY316 obtained by crossing PAY76 with PAY321 that were heterozygous for *EST2* (*EST2*/*est2Δ*) and carried the pRS415GAL or pRS413GAL::YRA1Δi plasmid. After 3 d of growth at 30°C, all of the spore colonies were transferred to 10 mL of liquid SRaf.

ChIP assays

Yeast mid-log cultures growing at 30°C were processed as described (Hecht and Grunstein 1999) with minor modifications. Cells were broken in a multibead shocker at 4°C in lysis buffer (50 mM HEPES-KOH at pH 7.5, 140 mM NaCl, 1 mM EDTA, 1% Triton X-100, 0.1% sodium deoxicholate). Chromatin was sonicated to an average fragment size of 400–500 bp and immunoprecipitated with 5 µL of anti-histone H2A (phospho-129) or anti-HA antibody coated to Protein A Dynabeads (Invitrogen).

Genome instability analysis in Saccharomyces cerevisiae

Spontaneous recombination frequencies were obtained as the average value of median frequencies obtained by six to 10 fluctuation tests performed with two to three independent transformants. For each fluctuation test, six independent colonies were analyzed as described previously (Prado and Aguilera 2005).

Downloaded from genesdev.cshlp.org on September 30, 2020 - Published by Cold Spring Harbor Laboratory Press

Senescence assays and telomere analysis

Senescence assays in liquid medium were performed as described previously (Churikov et al. 2014) from haploid spore products of diploid PAY247 or PAY249 obtained by crossing PAY267 or PAY269 with PAY76 that were heterozygous for *EST2* (*EST2*/*est2Δ*) and carried the pEST2-URA3 plasmid and the pRS413GAL or pRS413GAL::YRA1Δi plasmid. To ensure homogeneous telomere length before sporulation, the diploids were propagated for at least 50 generations on YPD plates. After 3 d of growth at 30°C, all of the spore colonies were transferred to 2 mL of liquid SGal-his to estimate the number of population doublings, and the suspensions were immediately diluted to 10^5 cells per milliliter. Cells were serially passaged in 15 mL of liquid SGal-his at 10^5 cells per milliliter at 48-h intervals. Replicative senescence was calculated as the average of two to 10 independent spores with identical genotype. Telomere analysis of the samples was performed as described (Churikov et al. 2014; Hardy et al. 2014).

Acknowledgments

We thank A. Greenleaf for generously providing the pET15-Yra1 plasmid for recombinant Yra1 purification, and E. Andújar and M. Pérez for technical assistance in the DRIP-seq experiments performed in the Genomic Unit of the Andalusian Center of Molecular Biology and Regenerative Medicine. Research was funded by grants from the European Research Council (ERC2014 AdG669898 TARLOOP), the Spanish Ministry of Economy and Competitiveness (BFU2016-75058-P), the Junta de Andalucía (PA12-BIO1238), and the European Union Regional Funds (FEDER) to A.A., and the Ligue Nationale Contre le Cancer (Équipe Labellisée) to V.G. P.A. was the recipient of Région Provence-Alpes-Côte d'Azur and Association pour la Recherche Contre le Cancer (ARC) predoctoral training grants.

Author contributions: M.G.-R., P.A. and A.G.R. performed all experiments, with the exception of the DRIP-seq and its bioinformatic analysis, which were performed by J.L.-B., and the construction of the head-on transcription–replication system, which was performed by J.F.R. The study was designed by M.G.-R., P.A., A.G.R., M.-N.S., V.G., and A.A. who also analyzed the data. A.G.-R. and A.A. wrote the first draft of the manuscript. All authors contributed to the final version.

References

Aguilera A, García-Muse T. 2012. R loops: from transcription byproducts to threats to genome stability. *Mol Cell* **46:** 115–124.

Arora R, Lee Y, Wischnewski H, Brun CM, Schwarz T, Azzalin CM. 2014. RNaseH1 regulates TERRA-telomeric DNA hybrids and telomere maintenance in ALT tumour cells. *Nat Commun* **5:** 5220.

Azzalin CM, Lingner J. 2015. Telomere functions grounding on TERRA firma. *Trends Cell Biol* **25:** 29–36.

Balk B, Maicher A, Dees M, Klermund J, Luke-Glaser S, Bender K, Luke B. 2013. Telomeric RNA–DNA hybrids affect telomere-length dynamics and senescence. *Nat Struct Mol Biol* **20:** 1199–1205.

Bermejo R, Capra T, Jossen R, Colosio A, Frattini C, Carotenuto W, Cocito A, Doksani Y, Klein H, Gomez-Gonzalez B, et al. 2011. The replication checkpoint protects fork stability by releasing transcribed genes from nuclear pores. *Cell* **146:** 233–246.

Bhatia V, Barroso SI, García-Rubio ML, Tumini E, Herrera-Moyano E, Aguilera A. 2014. BRCA2 prevents R-loop accumulation and associates with TREX-2 mRNA export factor PCID2. *Nature* **511:** 362–365.

Bonnet A, Palancade B. 2014. Regulation of mRNA trafficking by nuclear pore complexes. *Genes* **5:** 767–791.

Boubakri H, de Septenville AL, Viguera E, Michel B. 2010. The helicases DinG, Rep and UvrD cooperate to promote replication across transcription units in vivo. *EMBO J* **29:** 145–157.

Castellano-Pozo M, García-Muse T, Aguilera A. 2012. R-loops cause replication impairment and genome instability during meiosis. *EMBO Rep* **13:** 923–929.

Chan YA, Aristizabal MJ, Lu PY, Luo Z, Hamza A, Kobor MS, Stirling PC, Hieter P. 2014. Genome-wide profiling of yeast DNA:RNA hybrid prone sites with DRIP-chip. *PLoS Genet* **10:** e1004288.

Churikov D, Charifi F, Simon MN, Geli V. 2014. Rad59-facilitated acquisition of Y′ elements by short telomeres delays the onset of senescence. *PLoS Genet* **10:** e1004736.

Dominguez-Sanchez MS, Saez C, Japon MA, Aguilera A, Luna R. 2011. Differential expression of THOC1 and ALY mRNP biogenesis/export factors in human cancers. *BMC Cancer* **11:** 77.

Dong S, Li C, Zenklusen D, Singer RH, Jacobson A, He F. 2007. YRA1 autoregulation requires nuclear export and cytoplasmic Edc3p-mediated degradation of its pre-mRNA. *Mol Cell* **25:** 559–573.

El Hage A, Webb S, Kerr A, Tollervey D. 2014. Genome-wide distribution of RNA–DNA hybrids identifies RNase H targets in tRNA genes, retrotransposons and mitochondria. *PLoS Genet* **10:** e1004716.

Flynn RL, Centore RC, O'Sullivan RJ, Rai R, Tse A, Songyang Z, Chang S, Karlseder J, Zou L. 2011. TERRA and hnRNPA1 orchestrate an RPA-to-POT1 switch on telomeric single-stranded DNA. *Nature* **471:** 532–536.

Gan W, Guan Z, Liu J, Gui T, Shen K, Manley JL, Li X. 2011. R-loop-mediated genomic instability is caused by impairment of replication fork progression. *Genes Dev* **25:** 2041–2056.

García-Benítez F, Gaillard H, Aguilera A. 2017. Physical proximity of chromatin to nuclear pores prevents harmful R loop accumulation contributing to maintain genome stability. *Proc Natl Acad Sci* **114:** 10942–10947.

García-Muse T, Aguilera A. 2016. Transcription–replication conflicts: how they occur and how they are resolved. *Nat Rev Mol Cell Biol* **17:** 553–563.

García-Pichardo D, Canas JC, García-Rubio ML, Gomez-Gonzalez B, Rondón AG, Aguilera A. 2017. Histone mutants separate R loop formation from genome instability induction. *Mol Cell* **66:** 597–609.e5.

García-Rubio M, Huertas P, Gonzalez-Barrera S, Aguilera A. 2003. Recombinogenic effects of DNA-damaging agents are synergistically increased by transcription in *Saccharomyces cerevisiae*. New insights into transcription-associated recombination. *Genetics* **165:** 457–466.

García-Rubio ML, Perez-Calero C, Barroso SI, Tumini E, Herrera-Moyano E, Rosado IV, Aguilera A. 2015. The fanconi anemia pathway protects genome integrity from R-loops. *PLoS Genet* **11:** e1005674.

García-Rubio M, Barroso SI, Aguilera A. 2018. Detection of DNA–RNA hybrids in vivo. *Methods Mol Biol* **1672:** 347–361.

Gavaldá S, Santos-Pereira JM, García-Rubio ML, Luna R, Aguilera A. 2016. Excess of Yra1 RNA-binding factor causes transcription-dependent genome instability, replication impairment and telomere shortening. *PLoS Genet* **12:** e1005966.

Downloaded from genesdev.cshlp.org on September 30, 2020 - Published by Cold Spring Harbor Laboratory Press

Ginno PA, Lott PL, Christensen HC, Korf I, Chedin F. 2012. R-loop formation is a distinctive characteristic of unmethylated human CpG island promoters. *Mol Cell* **45:** 814–825.

Graf M, Bonetti D, Lockhart A, Serhal K, Kellner V, Maicher A, Jolivet P, Teixeira MT, Luke B. 2017. Telomere length determines TERRA and R-loop regulation through the cell cycle. *Cell* **170:** 72–85 e14.

Hamperl S, Bocek MJ, Saldivar JC, Swigut T, Cimprich KA. 2017. Transcription–replication conflict orientation modulates R-loop levels and activates distinct DNA damage responses. *Cell* **170:** 774–786 e719.

Hardy J, Churikov D, Geli V, Simon MN. 2014. Sgs1 and Sae2 promote telomere replication by limiting accumulation of ssDNA. *Nat Commun* **5:** 5004.

Hecht A, Grunstein M. 1999. Mapping DNA interaction sites of chromosomal proteins using immunoprecipitation and polymerase chain reaction. *Methods Enzymol* **304:** 399–414.

Johnson SA, Kim H, Erickson B, Bentley DL. 2011. The export factor Yra1 modulates mRNA 3′ end processing. *Nat Struct Mol Biol* **18:** 1164–1171.

Kitada T, Schleker T, Sperling AS, Xie W, Gasser SM, Grunstein M. 2011. γH2A is a component of yeast heterochromatin required for telomere elongation. *Cell Cycle* **10:** 293–300.

Kohler A, Hurt E. 2007. Exporting RNA from the nucleus to the cytoplasm. *Nat Rev Mol Cell Biol* **8:** 761–773.

Lang KS, Hall AN, Merrikh CN, Ragheb M, Tabakh H, Pollock AJ, Woodward JJ, Dreifus JE, Merrikh H. 2017. Replication-transcription conflicts generate R-loops that orchestrate bacterial stress survival and pathogenesis. *Cell* **170:** 787–799 e718.

Ma WK, Cloutier SC, Tran EJ. 2013. The DEAD-box protein Dbp2 functions with the RNA-binding protein Yra1 to promote mRNP assembly. *J Mol Biol* **425:** 3824–3838.

Ma WK, Paudel BP, Xing Z, Sabath IG, Rueda D, Tran EJ. 2016. Recruitment, duplex unwinding and protein-mediated inhibition of the dead-box RNA helicase Dbp2 at actively transcribed chromatin. *J Mol Biol* **428:** 1091–1106.

MacKellar AL, Greenleaf AL. 2011. Cotranscriptional association of mRNA export factor Yra1 with C-terminal domain of RNA polymerase II. *J Biol Chem* **286:** 36385–36395.

Madireddy A, Kosiyatrakul ST, Boisvert RA, Herrera-Moyano E, García-Rubio ML, Gerhardt J, Vuono EA, Owen N, Yan Z, Olson S, et al. 2016. FANCD2 facilitates replication through common fragile sites. *Mol Cell* **64:** 388–404.

Maicher A, Lockhart A, Luke B. 2014. Breaking new ground: digging into TERRA function. *Biochim Biophys Acta* **1839:** 387–394.

Mirkin EV, Mirkin SM. 2007. Replication fork stalling at natural impediments. *Microbiol Mol Biol Rev* **71:** 13–35.

Niño CA, Guet D, Gay A, Brutus S, Jourquin F, Mendiratta S, Salamero J, Gélia V, Dargemont C. 2016. Posttranslational marks control architectural and functional plasticity of the nuclear pore complex basket. *J Cell Biol* **212:** 167–180.

Nudler E. 2012. RNA polymerase backtracking in gene regulation and genome instability. *Cell* **149:** 1438–1445.

Pfeiffer V, Crittin J, Grolimund L, Lingner J. 2013. The THO complex component Thp2 counteracts telomeric R-loops and telomere shortening. *EMBO J* **32:** 2861–2871.

Prado F, Aguilera A. 2005. Impairment of replication fork progression mediates RNA PolII transcription-associated recombination. *EMBO J* **24:** 1267–1276.

Preker PJ, Guthrie C. 2006. Autoregulation of the mRNA export factor Yra1p requires inefficient splicing of its pre-mRNA. *RNA* **12:** 994–1006.

Ren Y, Schmiege P, Blobel G. 2017. Structural and biochemical analyses of the DEAD-box ATPase Sub2 in association with THO or Yra1. *Elife* **6:** e20070.

Rodríguez-Navarro S, Strasser K, Hurt E. 2002. An intron in the YRA1 gene is required to control Yra1 protein expression and mRNA export in yeast. *EMBO Rep* **3:** 438–442.

Salas-Armenteros I, Perez-Calero C, Bayona-Feliu A, Tumini E, Luna R, Aguilera A. 2017. Human THO-Sin3A interaction reveals new mechanisms to prevent R-loops that cause genome instability. *EMBO J* **36:** 3532–3547.

Santos-Pereira JM, Aguilera A. 2015. R loops: new modulators of genome dynamics and function. *Nat Rev Genet* **16:** 583–597.

Schwab RA, Nieminuszczy J, Shah F, Langton J, Lopez Martinez D, Liang CC, Cohn MA, Gibbons RJ, Deans AJ, Niedzwiedz W. 2015. The fanconi anemia pathway maintains genome stability by coordinating replication and transcription. *Mol Cell* **60:** 351–361.

Simon MN, Churikov D, Geli V. 2016. Replication stress as a source of telomere recombination during replicative senescence in *Saccharomyces cerevisiae*. *FEMS Yeast Res* **16:** fow085.

Sollier J, Cimprich KA. 2015. Breaking bad: R-loops and genome integrity. *Trends Cell Biol* **25:** 514–522.

Sollier J, Stork CT, García-Rubio ML, Paulsen RD, Aguilera A, Cimprich KA. 2014. Transcription-coupled nucleotide excision repair factors promote R-loop-induced genome instability. *Mol Cell* **56:** 777–785.

Strasser K, Hurt E. 2000. Yra1p, a conserved nuclear RNA-binding protein, interacts directly with Mex67p and is required for mRNA export. *EMBO J* **19:** 410–420.

Sun Q, Csorba T, Skourti-Stathaki K, Proudfoot NJ, Dean C. 2013. R-loop stabilization represses antisense transcription at the *Arabidopsis* FLC locus. *Science* **340:** 619–621.

Tuduri S, Crabbe L, Conti C, Tourriere H, Holtgreve-Grez H, Jauch A, Pantesco V, De Vos J, Thomas A, Theillet C, et al. 2009. Topoisomerase I suppresses genomic instability by preventing interference between replication and transcription. *Nat Cell Biol* **11:** 1315–1324.

Wahba L, Costantino L, Tan FJ, Zimmer A, Koshland D. 2016. S1-DRIP-seq identifies high expression and polyA tracts as major contributors to R-loop formation. *Genes Dev* **30:** 1327–1338.

Wellinger RE, Prado F, Aguilera A. 2006. Replication fork progression is impaired by transcription in hyperrecombinant yeast cells lacking a functional THO complex. *Mol Cell Biol* **26:** 3327–3334.

Yu TY, Kao YW, Lin JJ. 2014. Telomeric transcripts stimulate telomere recombination to suppress senescence in cells lacking telomerase. *Proc Natl Acad Sci* **111:** 3377–3382.

Downloaded from genesdev.cshlp.org on September 30, 2020 - Published by Cold Spring Harbor Laboratory Press

Yra1-bound RNA–DNA hybrids cause orientation-independent transcription–replication collisions and telomere instability

María García-Rubio, Paula Aguilera, Juan Lafuente-Barquero, et al.

Genes Dev. 2018, **32:** originally published online June 28, 2018
Access the most recent version at doi:10.1101/gad.311274.117

Supplemental Material http://genesdev.cshlp.org/content/suppl/2018/06/28/gad.311274.117.DC1

References This article cites 57 articles, 18 of which can be accessed free at: http://genesdev.cshlp.org/content/32/13-14/965.full.html#ref-list-1

Creative Commons License This article is distributed exclusively by Cold Spring Harbor Laboratory Press for the first six months after the full-issue publication date (see http://genesdev.cshlp.org/site/misc/terms.xhtml). After six months, it is available under a Creative Commons License (Attribution-NonCommercial 4.0 International), as described at http://creativecommons.org/licenses/by-nc/4.0/.

Email Alerting Service Receive free email alerts when new articles cite this article - sign up in the box at the top right corner of the article or **click here.**

© 2018 García-Rubio et al.; Published by Cold Spring Harbor Laboratory Press